Krüppel-like factor 6–mediated loss of BCAA catabolism contributes to kidney injury in mice and humans

Sian E. Piret[a], Yiqing Guo[a], Ahmed A. Attallah[a], Sylvia J. Horne[a], Amy Zollman[b], Daniel Owusu[a], Justina Henein[a], Viktoriya S. Sidorenko[c], Monica P. Revelo[d], Takashi Hato[b], Avi Ma'ayan[e], John Cijiang He[e,f,g], and Sandeep K. Mallipattu[a,h,1]

[a]Division of Nephrology, Department of Medicine, Stony Brook University, Stony Brook, NY 11794; [b]Department of Medicine, Indiana University, Indianapolis, IN 46202; [c]Department of Pharmacological Sciences, Stony Brook University, Stony Brook, NY 11794; [d]Department of Pathology, University of Utah, Salt Lake City, UT 84112; [e]Department of Pharmacological Sciences, Mount Sinai Center for Bioinformatics, Icahn School of Medicine at Mount Sinai, New York, NY 10029; [f]Division of Nephrology, Department of Medicine, Icahn School of Medicine at Mount Sinai, New York, NY 10029; [g]Renal Section, James J. Peters Veteran Affairs Medical Center, Bronx, NY 10468; and [h]Renal Section, Northport Veterans Affairs Medical Center, Northport, NY 11768

Edited by Martin R. Pollak, Beth Israel Deaconess Medical Center, Brookline, MA, and approved April 5, 2021 (received for review December 7, 2020)

Altered cellular metabolism in kidney proximal tubule (PT) cells plays a critical role in acute kidney injury (AKI). The transcription factor Krüppel-like factor 6 (KLF6) is rapidly and robustly induced early in the PT after AKI. We found that PT-specific *Klf6* knockdown (*Klf6*^{PTKD}) is protective against AKI and kidney fibrosis in mice. Combined RNA and chromatin immunoprecipitation sequencing analysis demonstrated that expression of genes encoding branched-chain amino acid (BCAA) catabolic enzymes was preserved in *Klf6*^{PTKD} mice, with KLF6 occupying the promoter region of these genes. Conversely, inducible *KLF6* overexpression suppressed expression of BCAA genes and exacerbated kidney injury and fibrosis in mice. In vitro, injured cells overexpressing *KLF6* had similar decreases in BCAA catabolic gene expression and were less able to utilize BCAA. Furthermore, knockdown of *BCKDHB*, which encodes one subunit of the rate-limiting enzyme in BCAA catabolism, resulted in reduced ATP production, while treatment with BCAA catabolism enhancer BT2 increased metabolism. Analysis of kidney function, *KLF6*, and BCAA gene expression in human chronic kidney disease patients showed significant inverse correlations between *KLF6* and both kidney function and BCAA expression. Thus, targeting KLF6-mediated suppression of BCAA catabolism may serve as a key therapeutic target in AKI and kidney fibrosis.

kidney | acute kidney injury | proximal tubule | transcription factor | branched-chain amino acids

Chronic kidney disease (CKD) causes significant morbidity and mortality and has a prevalence in the US adult population of ~15%. CKD can result from repeated bouts of acute kidney injury (AKI) attributable to environmental or toxic insults or be secondary to other diseases or their treatments. In majority of the cases, the proximal tubule (PT) is a primary site of damage in AKI, as the high metabolic activity of PT cells renders them susceptible to ischemic injury, and their role in excretion of drugs and toxins requires flux of potentially damaging agents through the PT cells (1). One such class of agent is DNA-damaging chemotherapeutics, which accumulate in PT cells, causing AKI and nephron loss. After injury, PT cells de-differentiate and secrete soluble factors such as Wnt and Hedgehog family members and cytokines (1–4). Surviving de-differentiated PT cells can re-enter the cell cycle and proliferate to repair the injured PT, followed by redifferentiation to fully functional PT cells (2). However, cells that instead undergo cell cycle arrest at the G2/M checkpoint may not recover, leading to atrophy and up-regulation of profibrotic signaling (5), triggering fibrosis by stimulating differentiation of resident fibroblasts to myofibroblasts that secrete extracellular matrix proteins, and recruiting immune cells such as macrophages and T cells (1).

In addition to inducing pathogenic signaling pathways, injured PT cells also demonstrate drastically altered cellular metabolism. Uninjured PT cells rely heavily on mitochondrial fatty acid β-oxidation, tricarboxylic acid (TCA) cycle, and oxidative phosphorylation for ATP production. However, in the setting of injury, fatty acid β-oxidation is suppressed, with only a modest compensatory up-regulation of glycolysis, such that overall ATP levels are reduced in injured PT (6). Furthermore, inhibition of fatty acid β-oxidation in vitro caused de-differentiation and apoptosis of tubular epithelial cells and in vivo worsened kidney injury after folic acid treatment (6). Interestingly, up-regulation of either mitochondrial fatty acid β-oxidation or peroxisomal fatty acid oxidation (FAO) can protect against kidney injury (6, 7), suggesting that preservation of cellular metabolism may be a therapeutic target in AKI. Transcriptomic studies in kidney biopsies with human CKD as well as after ischemia reperfusion injury (IRI) in mice demonstrate dysregulated fatty acid metabolism as well as amino acid metabolism (6, 8). Although the role of PT fatty acid β-oxidation has been previously described in AKI, the role of PT amino acid metabolism in AKI remains to be explored. Furthermore,

Significance

The kidney proximal tubule is particularly susceptible to acute injury, which results in loss of fatty acid oxidation (FAO), their primary energy source. Here, we show that loss of the transcription factor KLF6 specifically in the proximal tubule in mice protects against acute injury and fibrosis, with preservation of transcripts that mediate branched-chain amino acid (BCAA) catabolism, which were down-regulated in injured control mice. BCAA may provide tricarboxylic acid cycle intermediates in the absence of FAO, and we show that loss of BCAA catabolism in vitro resulted in decreased ATP production, while pharmacological activation of BCAA catabolism increased mitochondrial oxygen consumption. Thus, preservation of BCAA catabolism may be a possible therapeutic target in acute kidney injury.

Author contributions: S.E.P. and S.K.M. designed research; S.E.P., Y.G., A.A.A., S.J.H., A.Z., D.O., J.H., and V.S.S. performed research; S.E.P., M.P.R., A.M., and S.K.M. analyzed data; and S.E.P., T.H., A.M., J.C.H., and S.K.M. wrote the paper.

Competing interest statement: J.C.H. declares a Shangpharma research grant of $250,000 per year in 2019 to 2020 and is a Scientific Advisory Board member for RenalytixAI.

This article is a PNAS Direct Submission.

[1]To whom correspondence may be addressed. Email: sandeep.mallipattu@stonybrookmedicine.edu.

This article contains supporting information online at https://www.pnas.org/lookup/suppl/doi:10.1073/pnas.2024414118/-/DCSupplemental.

Published May 31, 2021.

the mechanisms of PT injury described to date have largely been explored using mouse models with knock-out and overexpression of individual signaling molecules, but mechanisms by which global pathways, both fibrotic/inflammatory and metabolic, and the switch between normal recovery and atrophy are regulated in AKI are not well characterized.

Transcription factors act as master regulators of fundamental biological processes, due to their ability to regulate the expression of multiple downstream targets and form feedback loops. In AKI, well-studied transcription factors such as FOS and JUN family members are highly up-regulated. Recent studies of molecular responses to IRI in human samples and PT translational profiling after unilateral ureteric obstruction (UUO) in mice also identified the zinc-finger transcription factor Krüppel-like factor 6 (KLF6) as a similar early injury response gene (9, 10). KLFs comprise a family of zinc-finger transcription factors with highly conserved C-terminal DNA-binding domains and variable N termini that are widely expressed, including in the kidney (11). KLF6 has roles in multiple processes such as cell proliferation and differentiation, apoptosis, DNA damage responses, and mitochondrial function (12) and has been identified to play roles in hepatic, cardiac, and kidney fibrosis, with context-dependent effects (13, 14). Within the kidney, KLF6 is expressed in glomerular podocytes and is an essential regulator of mitochondrial function in the setting of focal segmental glomerulosclerosis (FSGS) (15). In addition to its expression in glomerular podocytes, KLF6 is also variably expressed in the PT, but its role in PT cells, either in normal function or after injury, is not understood. Overexpression of KLF6 in HK-2 cells resulted in a de-differentiated phenotype with decreased E-cadherin and increased vimentin expression and also led to increased expression of macrophage inflammatory protein-3α (16). In addition, KLF6 expression increased in response to high glucose, and this effect was blocked by knockdown of *TGFB1* or treatment with TGF-β1 neutralizing antibody. Direct treatment with TGF-β1 also induced KLF6 expression, indicating a possible positive feedback loop in HK-2 cells (16). KLF6 has also been shown to be induced in cancer cells in vitro by subapoptotic doses of the DNA-damaging chemotherapeutic drug cisplatin (17). In order to determine the role of PT KLF6 in response to DNA damage, we used the naturally occurring toxin aristolochic acid I (AAI). AAI-associated nephropathy is clinically relevant (18), and AAI toxicity is highly specific to the PT, thus allowing the study of the role of PT KLF6 specifically in response to PT injury. Furthermore, AAI reliably causes both AKI and a transition to fibrosis in mice, in contrast to most cisplatin regimens (19). AAI enters PT cells via basolateral organic anion transporters (OATs) 1 to 3 and has both genotoxic effects, via formation of aristolactam (AL)-DNA adducts, and cytotoxic effects, causing mitochondrial damage, which generates reactive oxygen species, and specifically inhibiting normal PT functions such as receptor-mediated endocytosis (18–20). Here, we demonstrate through modulation of KLF6 expression specifically in the PT through gain-of-function and loss-of-function studies in mice that KLF6-mediated suppression of branched-chain amino acid (BCAA) catabolism contributes to AKI and ensuing kidney fibrosis.

Results

AAI Treatment Increases Renal PT *Klf6* Expression. Since several members of the KLF family are expressed in the epithelial cells in the kidney (21), we initially undertook qRT-PCR for these epithelial *Klfs* in kidney cortex harvested 24 h after a single dose of PT-specific toxin, AAI, versus vehicle (dimethyl sulfoxide [DMSO]) in C57BL/6 mice. *Klf4*, *Klf5*, and *Klf6* were significantly up-regulated, while *Klf15* was significantly down-regulated (Fig. 1*A*), and these changes in gene expression occurred prior to a significant rise in serum creatinine (Fig. 1*B*). To determine whether *Klf6* up-regulation is transient or prolonged, we administered AAI in multiple injections 3 d apart for either two injections or 3 wk (active phase) or for 3 wk followed by 3 wk without AAI (remodeling phase) (Fig. 1*C*). PT remained intact 24 h after one injection, but after two injections, PT cells underwent cell death, and mice treated with multiple AAI doses demonstrated loss of PT, inflammatory infiltrates, protein casts, and fibrosis at the end of the remodeling phase (Fig. 1*D*). *Klf6* expression remained significantly elevated in the active and remodeling phases of injury (Fig. 1*E*), suggesting a role for KLF6 throughout the acute and fibrotic phases of injury. KLF6 is expressed in glomerular, tubular, and inflammatory cells, and to determine the contribution of PT-specific *Klf6* expression to the observed increase in renal cortical *Klf6* expression, we undertook RNA sequencing (RNA-seq) in microdissected S2/S3 PT segments 24 h after one AAI injection, prior to loss of PT cells. *Klf6* was highly up-regulated at a level comparable to the well-known early response transcription factors *Fos* and *Jun*, indicating that the early induction of *Klf6* messenger RNA (mRNA) expression in the kidney is driven by its expression in PT cells (Fig. 1*F*). These findings are consistent with recently published single-cell/nuclear RNA-seq data showing up-regulation of *Klf6* in PT cells in injured mouse and human kidneys (22, 23). Finally, data mining of expression arrays from previously reported IRI time course studies (8) confirmed the early induction in KLF6 expression, within 2 h of AKI, similarly to *Fos* and *Jun* (Fig. 1*G*). These data suggest that *Klf6* is an early inducible injury response gene after treatment with the PT-specific toxin AAI and after IRI and remains elevated despite the cessation of the AAI.

PT-Specific Loss of KLF6 Attenuates Kidney Injury in the Active and Remodeling Phases Post-AAI Treatment. To determine the contribution of PT-specific KLF6 to AAI-induced injury, we generated mice with PT-specific knockdown of *Klf6* ($Klf6^{PTKD}$) by crossing $Klf6^{fl/fl}$ mice (24) with *Pepck*-Cre mice (25). $Klf6^{PTKD}$ mice were viable and fertile, with significant knockdown of PT-specific KLF6 protein expression but no change in *Klf6* mRNA expression in liver, as compared to $Klf6^{fl/fl}$ mice (*SI Appendix*, Fig. S1 *A–C*). There were no overt differences in kidney histology or function between $Klf6^{fl/fl}$ and $Klf6^{PTKD}$ mice at 24 wk of age (*SI Appendix*, Fig. S1 *D* and *E*), and expression levels of OATs 1 to 3 (*Slc22a6*, *Slc22a7*, and *Slc22a8*), route of AAI PT entry, were not significantly different (*SI Appendix*, Fig. S1*F*).

Control ($Klf6^{fl/fl}$) and $Klf6^{PTKD}$ mice were treated with vehicle (DMSO) or 3 mg/kg AAI intraperitoneally every 3 d for 3 wk and euthanized 3 d after the last AAI injection to assess the active phase of injury or 3 wk after the last AAI injection to assess the remodeling phase of injury (Fig. 1*C*). $Klf6^{fl/fl}$ and $Klf6^{PTKD}$ mice had similar quantities of AL-DNA adducts both after one injection and at the end of the active and remodeling phases (*SI Appendix*, Fig. S1 *G* and *H*), suggesting similar PT uptake of AAI and repair of AL-DNA adducts in $Klf6^{fl/fl}$ and $Klf6^{PTKD}$ mice. While undergoing injections, mice receiving AAI lost weight relative to those receiving DMSO, with a similar reduction of ∼18% from baseline in both $Klf6^{fl/fl}$ and $Klf6^{PTKD}$ mice at the final injection of AAI, followed by regaining of similar amounts of body weight (*SI Appendix*, Fig. S2*A*). Kidney weights relative to starting (day 0) body weight were similar between DMSO- and AAI-treated $Klf6^{fl/fl}$ and $Klf6^{PTKD}$ mice at the end of the active phase (*SI Appendix*, Fig. S2*B*). In the remodeling phase, kidneys from AAI-treated $Klf6^{fl/fl}$ mice weighed significantly less than those from DMSO-treated mice, but in AAI-treated $Klf6^{PTKD}$ mice, kidney weights were preserved (*SI Appendix*, Fig. S2*B*). Kidney function was assessed by measuring serum creatinine (Fig. 2*A*) and urea nitrogen (Fig. 2*B*) concentrations. Both serum creatinine and urea nitrogen concentrations were significantly elevated in mice receiving AAI versus DMSO; however, the elevations were significantly less in $Klf6^{PTKD}$ mice compared to $Klf6^{fl/fl}$ mice (Fig. 2 *A* and *B*). Histological analysis using hematoxylin and eosin and periodic acid Schiff staining showed that both $Klf6^{fl/fl}$ and $Klf6^{PTKD}$ mice treated with AAI had shedding tubules with remnant basement membranes, inflammatory infiltrates that were predominantly localized in the

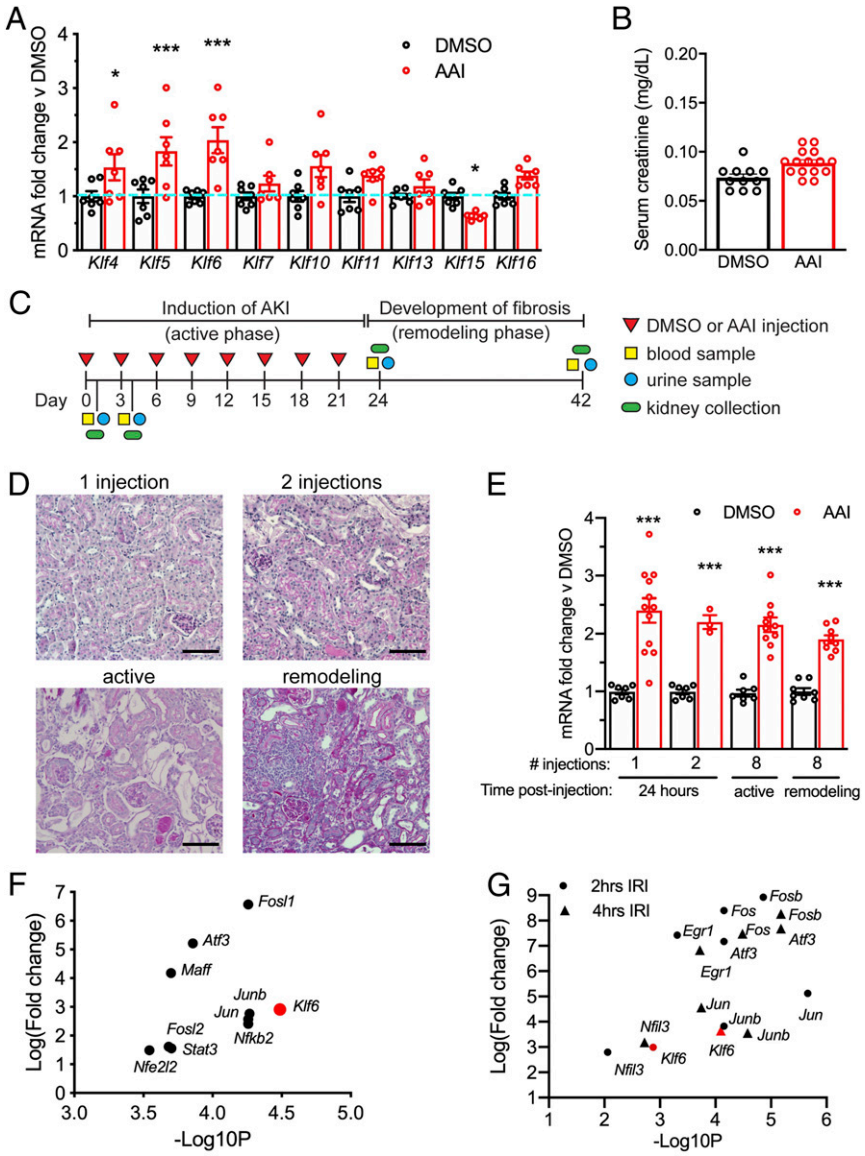

Fig. 1. *Klf6* expression is highly up-regulated early in kidney injury. (*A*) qRT-PCR analysis of epithelial expressed *Klf*s in kidney cortex 24 h after injection of AAI versus mice injected with DMSO (vehicle). $n = 7$ mice per group; $^{*}P < 0.05$; $^{***}P < 0.001$, *t* test with Holm–Sidak correction for multiple comparisons. (*B*) Serum creatinine concentrations 24 h after injection of DMSO or AAI. (*C*) Protocol for DMSO/AAI treatments in mice. (*D*) Periodic acid Schiff staining of kidneys from mice treated with AAI for one or two injections or eight injections in the active and remodeling phases. (Scale bars, 100 μm.) (*E*) qRT-PCR analysis of *Klf6* expression in the kidney cortex after a series of injections administered every 3 d. DMSO controls for one and two injections are the same mice, given one injection of DMSO. $n = 3$ to 12 mice per group; $^{***}P < 0.001$; *t* test with Holm–Sidak correction for multiple comparisons. (*F*) Top 10 up-regulated transcription factors in microdissected S2/S3 PT segments 24 h after 1 AAI injection compared to DMSO, as assessed by RNA-seq. $n = 3$ mice per group. Data are mean ± SEM with *n* indicating the number of biological replicates. (*G*) Previously reported RNA-seq data from Liu et al. (8) was used to identify the eight most highly up-regulated transcription factors in kidney cortex 2 h (circles) and 4 h (triangles) after IRI compared to sham-operated mice.

outer cortex, and multiple protein casts in both the cortex and medulla (Fig. 2 *C* and *D*). However, these features were less severe in *Klf6*^{PTKD} mice compared to *Klf6*$^{fl/fl}$ mice, with preservation of tubules and smaller inflammatory infiltrates. Analysis of PT area was undertaken using fluorescent Lotus lectin staining to identify intact PT brush borders in fully differentiated PT cells and immunofluorescence for cytokeratin-20 (KRT-20) to identify injured PTs (8). Compared to mice treated with DMSO, both *Klf6*$^{fl/fl}$ and *Klf6*^{PTKD} mice treated with AAI had significant loss of mature PT, as shown by loss of Lotus lectin staining, and induction of KRT-20 expression, indicating PT damage in both the active and remodeling phases (Fig. 2*E* and *SI Appendix*, Fig. S2*C*). *Klf6*^{PTKD} mice treated with AAI had significant preservation of mature PT compared to *Klf6*$^{fl/fl}$ mice, accompanied by similar levels of KRT-20 induction in both the active and remodeling phases.

Trichrome staining of remodeling phase kidneys showed extensive deposition of fibrotic material in *Klf6*$^{fl/fl}$ mice, with significantly less fibrosis in *Klf6*^{PTKD} mice (Fig. 2*F*, blue staining; *SI Appendix*, Table S1). Deposition of the fibrotic matrix component collagen I, detected using immunofluorescence (Fig. 2*G* and *SI Appendix*, Fig. S2*D*), showed that collagen I was significantly increased in *Klf6*$^{fl/fl}$ mice with AAI but not in *Klf6*^{PTKD} mice with AAI compared to DMSO in the active phase. In the remodeling phase, collagen I was significantly increased in *Klf6*$^{fl/fl}$ and *Klf6*^{PTKD} mice with AAI, with a significantly lower percentage area in *Klf6*^{PTKD} mice with AAI compared to *Klf6*$^{fl/fl}$ mice with AAI. Interstitial inflammatory cells consisting of CD68^{+} macrophages and GR-1^{+} myeloid monocytes were present in *Klf6*$^{fl/fl}$

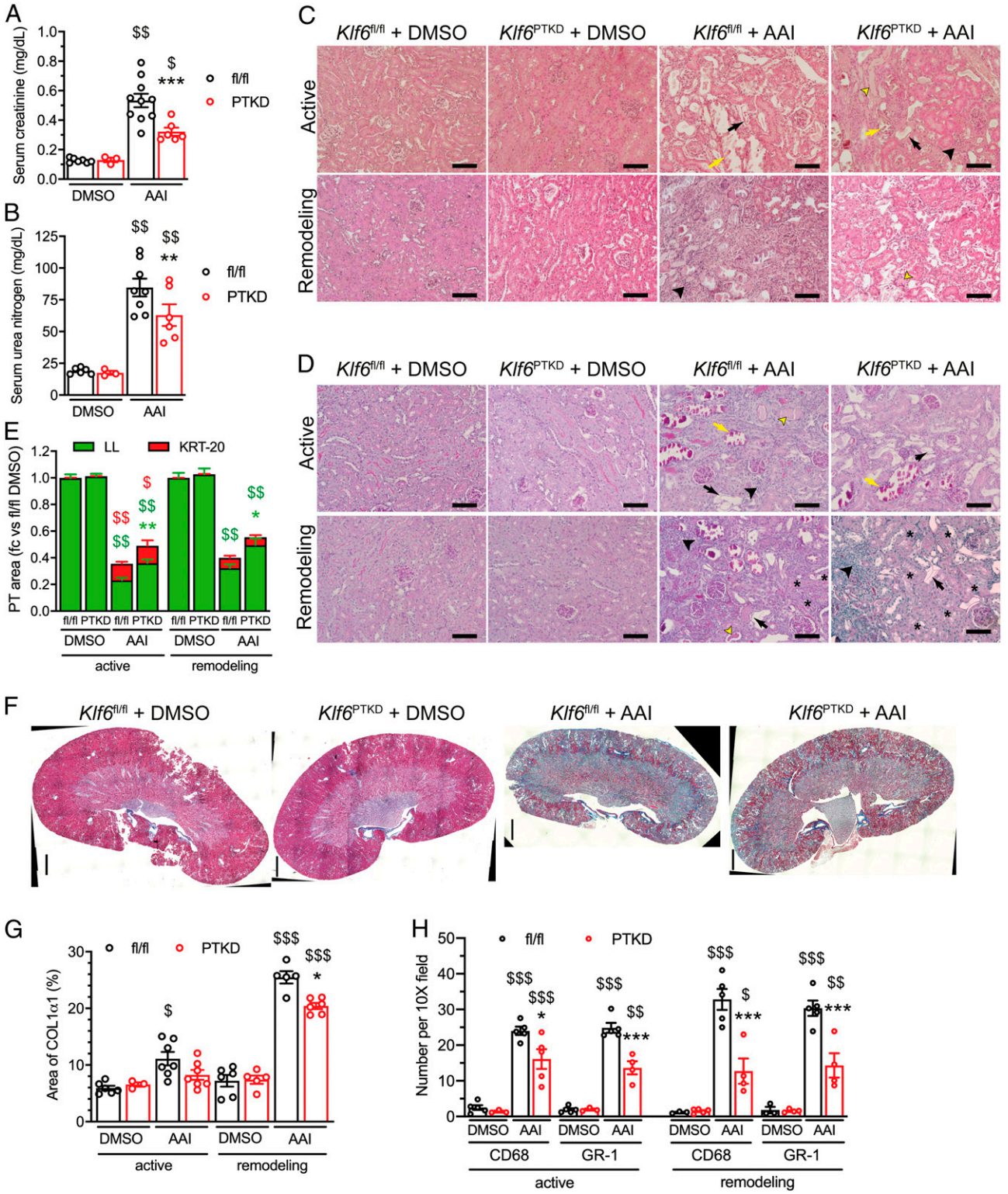

Fig. 2. AAI-treated *Klf6*^{PTKD} mice have preserved kidney function and reduced injury, fibrosis, and inflammation. Mice were injected with DMSO or AAI every 3 d for 3 wk and euthanized 3 d (active phase) or 3 wk (remodeling phase) after the last injection. (*A* and *B*) Serum creatinine (*A*) and urea nitrogen (*B*) concentrations in the active phase. (*C* and *D*) Histological analysis of kidneys using hematoxylin and eosin (*C*) and periodic acid Schiff (*D*) stains. Yellow arrows: shedding tubules; black arrows: remnant basement membranes; yellow arrowheads: protein casts; black arrowheads: inflammatory infiltrates; and asterisks: preserved PT with brush border (scale bars, 100 μm.) (*E*) Quantification of immunofluorescent staining for cytokeratin-20 (KRT-20) as a marker of injured PT and Lotus lectin (LL) as a marker of uninjured PT. (*F*) Histological analysis of kidney fibrosis using Masson's trichrome stain. (Scale bars, 1 mm.) (*G*) Quantification of area stained for fibrotic marker COL1α1. (*H*) Quantification of number of CD68 and GR-1 positive immune cells per field. $n = 3$ to 10 per group; $^{\$}P < 0.05$, $^{\$\$}P < 0.01$, $^{\$\$\$}P < 0.001$ versus same genotype with DMSO; $^{*}P < 0.05$, $^{**}P < 0.01$, $^{***}P < 0.001$ versus *Klf6*$^{fl/fl}$ with AAI; one-way ANOVA with Sidak's correction for multiple testing. Data are mean ± SEM with *n* indicating the number of biological replicates.

and *Klf6*^{PTKD} mice treated with AAI but were significantly less abundant in *Klf6*^{PTKD} mice in both the active and remodeling phases (Fig. 2*H*). Thus, loss of PT-specific KLF6 protects against AAI-induced PT injury, fibrosis, and inflammation, despite the presence of similar quantities of AL-DNA adducts compared to AAI-treated control mice.

PT-Specific Loss of KLF6 Reduces Inflammatory Signaling and Preserves Cellular Metabolism after AAI Treatment. We sought to understand the mechanisms by which loss of PT KLF6 protects against injury, and we therefore undertook RNA-seq of kidney cortex in *Klf6*$^{fl/fl}$ and *Klf6*^{PTKD} mice treated with DMSO or AAI in the active phase or remodeling phase. Significantly differentially expressed genes were defined as having a >1.5- or <0.67-fold change and false discovery rate of <0.05 in any given pairwise genotype or treatment comparison. A combined total of 7,673 genes were found to be differentially expressed as a result of all the pairwise comparisons, and hierarchical clustering showed these to group into two main clusters: genes that were induced in response to AAI treatment and genes that were suppressed in response to AAI treatment (*SI Appendix*, Fig. S3*A* and Dataset S1). Unbiased analysis of transcriptional effects of AAI treatment in *Klf6*$^{fl/fl}$ mice by undertaking pathway enrichment analysis showed that the most significantly up-regulated pathways were predominantly inflammatory and ECM/cell adhesion pathways (e.g., cytokine/chemokine signaling) and integrin/focal adhesion pathways, respectively (*SI Appendix*, Fig. S3 *B* and *C*). Markers of cellular senescence, including components of the senescence-associated secretory phenotype, were also up-regulated after AAI treatment (*SI Appendix*, Fig. S3*D*), but the overall pathway was not differentially expressed between *Klf6*$^{fl/fl}$ and *Klf6*^{PTKD} mice. In general, these pathways were less significantly up-regulated in the remodeling phase compared to the active phase. The most significantly down-regulated pathways after AAI were metabolic pathways, including fatty acid– and amino acid–related pathways; these pathways were similarly or slightly less significantly decreased in the remodeling phase compared to the active phase (*SI Appendix*, Fig. S3 *B*, *E*, and *F*). Similar to other studies, genes encoding enzymes involved in anerobic glycolysis were up-regulated after AAI (26, 27) (*SI Appendix*, Fig. S3*F*).

To determine pathways potentially directly and indirectly regulated by KLF6, we further analyzed the differentially expressed genes by classifying them based on the presence and location of KLF6 binding sites, using KLF6 chromatin immunoprecipitation-sequencing (ChIP-Seq) data from the Encyclopedia of DNA Elements project. Class 2 genes were defined as having at least 1 KLF6 binding site within ±1 kb of the transcription start site (TSS), class 1 genes as having at least 1 KLF6 binding site between ±1 and 10 kb of the TSS and class 0 genes as having no KLF6 binding site within ±10 kb of the TSS. There were 538 genes that were both up-regulated in *Klf6*$^{fl/fl}$ mice and significantly down-regulated in *Klf6*^{PTKD} versus *Klf6*$^{fl/fl}$ mice in the active phase. Pathway enrichment analysis of these 538 genes showed that innate immune (e.g., TYROBP, phagosome, and macrophage)-related and cell adhesion (e.g., integrin, focal adhesion)–related pathways were significantly enriched (Fig. 3*A*). Classification of the genes according to KLF6 binding sites showed that the majority of DEGs (428/538) did not have KLF6 binding sites (class 0), and enrichment analysis of class 2 genes (72) and class 0 genes separately showed that the significance of these pathways was strongly driven by class 0 genes, indicating that the lower expression of these genes in *Klf6*^{PTKD} mice was likely an indirect effect of less PT injury as a result of PT-specific *Klf6* knockdown (Fig. 3*A*).

There were 388 genes that were both down-regulated in *Klf6*$^{fl/fl}$ mice and significantly preserved (up-regulated) in *Klf6*^{PTKD} versus *Klf6*$^{fl/fl}$ mice. Pathway enrichment analysis showed that these genes represented metabolic pathways, with amino acid metabolism and fatty acid metabolism being prominent (Fig. 3*B* and *SI Appendix*, Fig. S4). Enrichment analysis of the class 2 genes (103) and class 0 genes (246) showed that despite only ~25% of the genes having KLF6 binding sites within ±1 kb of the TSS (class 2), this subset of genes was the driver for the highly significant *P* values of these pathways. Strikingly, specific amino acid (Val, Leu, and Ile [BCAA] and Gly, Ser, and Thr) metabolic pathways were equally significant when only class 2 genes were analyzed, suggesting potential direct regulation of these pathways by KLF6 (Fig. 3*B*). By contrast, the high significance of fatty acid metabolic pathways and PPAR signaling pathway were largely driven by class 0 genes, suggesting indirect preservation of these pathways as a result of PT-specific *Klf6* knockdown. Gene-set enrichment analysis for specific Kyoto Encyclopedia of Genes and Genomes (KEGG) metabolic pathways (fatty acid degradation, amino acid metabolism, TCA cycle, and glycolysis) using all differentially regulated genes confirmed these to be significantly up-regulated (preserved) in *Klf6*^{PTKD} versus *Klf6*$^{fl/fl}$ mice (Fig. 3*C*).

Induction of KLF6 Exacerbates Kidney Injury and Suppresses BCAA Catabolic Genes Post-AAI Treatment. To determine whether overexpression of KLF6 would have the opposite effects, we used the "tet-on" system to generate a mouse model with doxycycline (DOX)-inducible expression of human KLF6 (h*KLF6*^{OE}; double transgenic CAG-*rtTA*,TRE-h*KLF6* mice) (*SI Appendix*, Fig. S5*A*). h*KLF6*^{OE} mice had robust induction of h*KLF6* expression after supplementation of diet with DOX for 7 d with no significant differences in mouse *Klf6* expression (*SI Appendix*, Fig. S5*B*), and the kidneys did not display overt histological injury or loss of kidney function after continuous treatment with DOX for 15 wk (*SI Appendix*, Fig. S5 *C* and *D*) compared to control mice (TRE-h*KLF6* with DOX treatment). However, to elicit whether induction of h*KLF6* in PT exacerbated AKI and kidney fibrosis, h*KLF6*^{OE} and control mice were treated with a lower dose of 1 mg/kg AAI or DMSO every 3 d for 2 wk followed by euthanasia after 3 further days (active phase) or 2 further weeks (remodeling phase) (*SI Appendix*, Fig. S6*A*). Control and h*KLF6*^{OE} mice receiving AAI lost similar amounts of body weight (*SI Appendix*, Fig. S6*B*) and kidney weights were similar between all groups (*SI Appendix*, Fig. S6*C*). h*KLF6*^{OE} mice had significantly elevated serum creatinine and urea nitrogen compared to control mice after AAI treatment in the active phase (Fig. 4 *A* and *B*). This was accompanied by loss of mature PT with a higher proportion of KRT-20–positive PT, which was exacerbated in h*KLF6*^{OE} mice at both time points (Fig. 4 *C*–*E* and *SI Appendix*, Fig. S6*D*) and increased fibrosis in both phases (Fig. 4*F* and *SI Appendix*, Fig. S6*E*). qRT-PCR analysis of genes encoding enzymes in the BCAA metabolic pathway showed suppression of BCAA genes after AAI treatment in control and h*KLF6*^{OE} mice, with further suppression in h*KLF6*^{OE} mice compared to control mice (Fig. 4*G*). Furthermore, expression of several of the BCAA genes were also either significantly reduced (*Hibch*) or showed a trend toward lower expression in h*KLF6*^{OE} versus control mice even without AAI treatment (DMSO treated) (Fig. 4*G*). These data suggest that induction of h*KLF6* in adult mice renders the kidney more susceptible to AKI and eventual fibrosis with significant dysregulation of genes encoding BCAA catabolism.

Induction of KLF6 Suppresses BCAA Catabolism, which Is an Important Substrate for ATP Production In Vitro. Mitochondrial BCAA catabolism can contribute to oxidative phosphorylation by production of acetyl-CoA and succinyl-CoA (*SI Appendix*, Fig. S4*B*). To investigate whether KLF6 regulates BCAA and cellular metabolism in vitro, we first assessed the expression of BCAA metabolic genes in HK-2 cells with overexpression of KLF6 (*KLF6*-OE), with or without AAI treatment. As in the h*KLF6*^{OE} mice, overexpression of KLF6 in HK-2 cells alone led to a trend toward suppression of several genes encoding BCAA enzymes, notably *BCKDHB*. Treatment of control *KLF6*-Con cells with 25 μM AAI for 6 h significantly suppressed expression of several enzymes, and these were further suppressed in *KLF6*-OE cells treated with AAI (Fig. 5*A*). To

MEDICAL SCIENCES

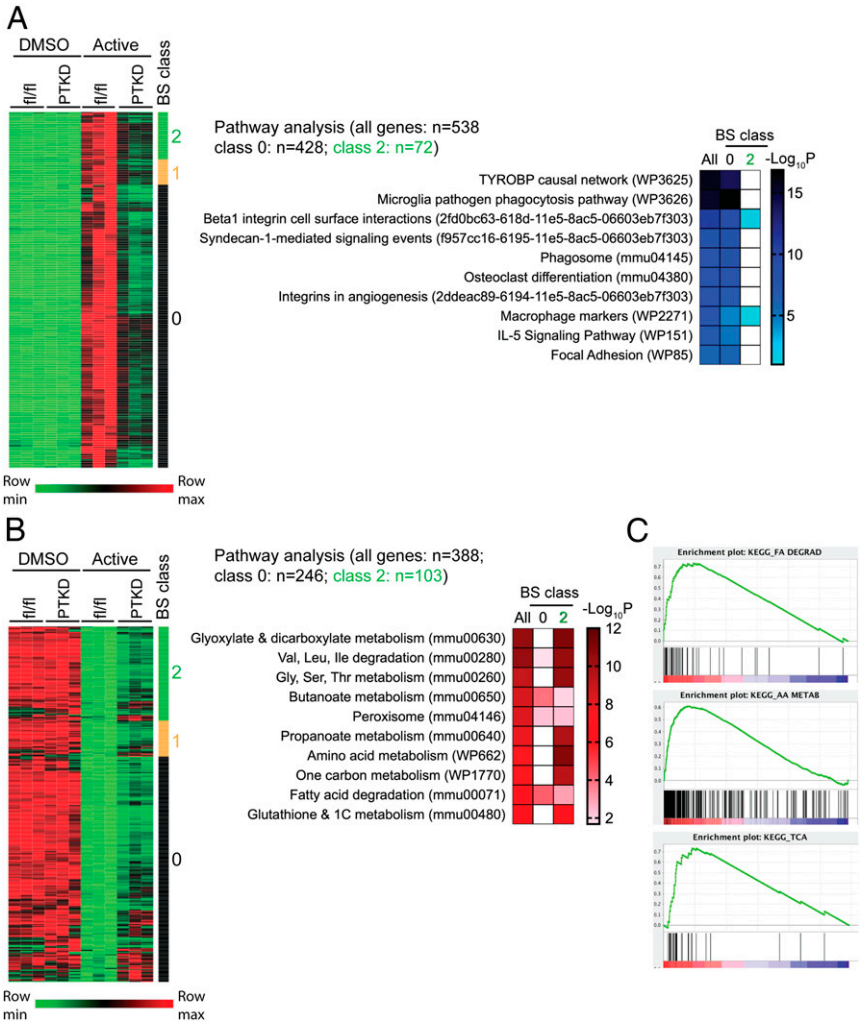

Fig. 3. Loss of KLF6 suppresses profibrotic pathways and preserves metabolic pathways after AAI treatment. (*A*) Classification and pathway enrichment analysis of genes up-regulated in *Klf6*$^{fl/fl}$ mice after AAI but significantly less up-regulated in *Klf6*^{PTKD} mice after AAI according to binding site class: class 2 with ≥1 KLF6 binding site within ±1 kb of TSS; class 1 with ≥1 KLF6 binding site at ±1 to 10 kb from TSS; and class 0 with no KLF6 binding site within ± 10 kb from TSS. (*B*) Classification and pathway enrichment analysis of genes down-regulated in *Klf6*$^{fl/fl}$ mice after AAI but significantly less down-regulated (i.e., preserved) in *Klf6*^{PTKD} mice after AAI according to binding site class: class 2 with ≥1 KLF6 binding site within ±1 kb of TSS; class 1 with ≥1 KLF6 binding site at ±1 to 10 kb from TSS; and class 0 with no KLF6 binding site within ±10 kb from TSS. (*C*) Gene-set enrichment analysis plots using all differentially expressed genes, for KEGG fatty acid degradation (FA DEGRAD), amino acid metabolism (AA METAB), and TCA cycle (KEGG_TCA).

determine whether this suppression in BCAA gene expression in the presence of AAI led to changes in BCAA catabolism, we measured intracellular BCAA concentrations. After treatment with AAI, *KLF6*-Con cells showed a decrease in BCAA, consistent with increased catabolism of the BCAA, potentially as a compensation for loss of FA oxidation (Fig. 5*B*). However, this effect was lost in *KLF6*-OE cells, which did not have a decrease in intracellular BCAA after AAI treatment, consistent with reduced ability to catabolize BCAA (Fig. 5*B*), and this correlated with reduced mitochondrial ATP production compared to AAI-treated *KLF6*-Con cells (Fig. 5*C*).

The standard media used to measure ATP production contains high concentrations of glucose (10 mM glucose, 1 mM glutamine, and 2 mM pyruvate), and to determine whether *KLF6* overexpression alone could alter the use of different energy sources, we instead undertook assays of oxygen consumption rate (OCR) in energy-restricted media (serum-free media with 1 mM glucose, no glutamine, and no pyruvate). *KLF6*-OE cells had reduced mitochondrial OCR (defined as initial OCR minus nonmitochondrial OCR determined after administration of rotenone/antimycin A) but had similar compensation after blocking glycolysis with 2-deoxyglucose (2-DG) and similar FAO (reduction in OCR after blocking FAO with etomoxir) (Fig. 5 *D* and *E*). Since the mitochondrial response to loss of glycolysis and the OCR resulting from FA oxidation were not changed in *KLF6*-OE cells, this suggested that overall mitochondrial function was not affected, but rather an inability to use BCAA as a source may account for the baseline reduction in mitochondrial OCR in these energy-restricted conditions. To determine whether loss of BCAA catabolism would lead to decreased mitochondrial ATP production, we generated HK-2 cells with knockdown of *BCKDHB* (*SI Appendix*, Fig. S7). *BCKDHA* and *BCKDHB* encode two of the subunits of the large protein complex branched-chain ketoacid dehydrogenase (BCKDH), which catalyzes the first irreversible and rate-limiting step in BCAA catabolism and is inhibited by phosphorylation by BCKDH kinase (BCKDK) (28). To shift the control *BCKDHB*-SCR and knockdown *BCKDHB*-sh cells toward mitochondrial ATP production, they were preincubated in 2-DG to block glycolysis for 1 h prior to undertaking the ATP Production Rate assay. Knockdown of *BCKDHB* resulted in a significant decrease in ATP production, showing that BCAA are used to generate ATP in human kidney cells (Fig. 5*F*). Conversely, to

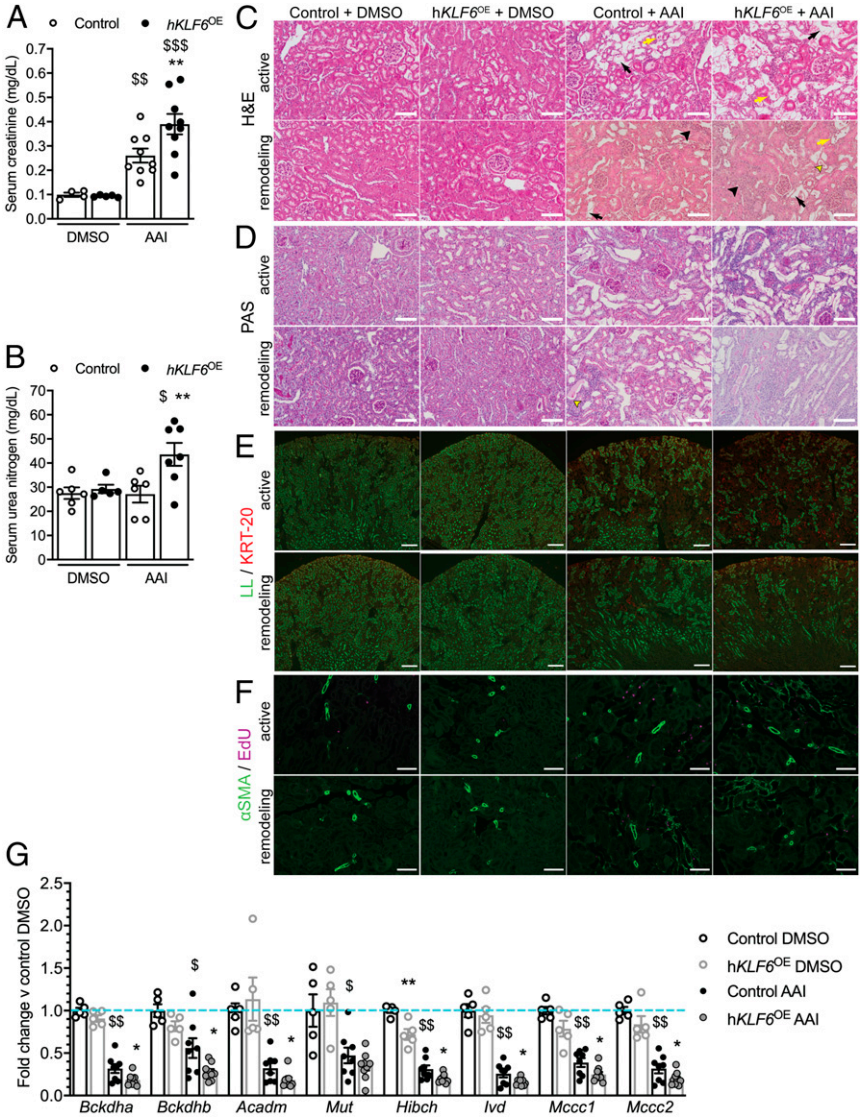

Fig. 4. h*KLF6*^{OE} mice have exacerbated kidney injury with suppression of BCAA genes. (*A* and *B*) Serum creatinine (*A*) and urea nitrogen (*B*) concentrations in control and h*KLF6*^{OE} mice treated with DMSO or AAI in the active phase. $n = 4$ to 9 per group; $^{\$}P < 0.05$, $^{\$\$}P < 0.01$, $^{\$\$\$}P < 0.001$ versus same genotype with DMSO; $^{**}P < 0.01$ versus control with AAI; one-way ANOVA with Sidak correction for multiple testing. (*C* and *D*) Representative histological images stained using hematoxylin and eosin (*C*) and periodic acid Schiff (*D*) stains. Yellow arrows: shedding tubules; black arrows: remnant basement membranes; yellow arrowheads: protein casts; and black arrowheads: inflammatory infiltrates. (Scale bars, 100 μm.) (*E*) Immunofluorescent staining for cytokeratin-20 (KRT-20) as a marker of injured PT (red) with costaining with Lotus lectin (LL) as a marker of uninjured PT (green). (Scale bars, 250 μm.) (*F*) Immunofluorescent staining for α-SMA (green) with costaining for EdU (magenta). (Scale bars, 100 μm.) (*G*) mRNA expression of BCAA genes in control and h*KLF6*^{OE} mice treated with DMSO or AAI in the active phase. $n = 5$ to 9 per group; $^{\$}P < 0.01$, $^{\$\$}P < 0.001$ versus control with DMSO; all h*KLF6*^{OE} with AAI are $P < 0.001$ versus h*KLF6*^{OE} with DMSO; $^{*}P < 0.05$, $^{**}P < 0.01$, $^{***}P < 0.001$ versus control with same treatment; multiple *t* tests with false discovery rate correction using the two-stage step-up model of Benjamini, Kreiger, and Yekutieli. Data are mean ± SEM with *n* indicating the number of biological replicates.

enhance BCAA catabolism, we treated HK-2 cells with BT2, which inhibits BCKDK, thus blocking the inhibitory phosphorylation of BCKDH. Under energy-restricted conditions, treatment with BT2 increased the OCR in DMSO-treated cells, which was sustained after inhibition of glycolysis and not due to alteration of FAO or non-mitochondrial OCR (Fig. 5 *G* and *H*). These findings indicate that KLF6-mediated suppression of BCAA catabolism reduces mitochondrial ATP production, which would likely exacerbate PT injury in the setting of cell stress, in which similarly energy-restricted conditions exist due to FAO being compromised.

BCAA Gene Expression Is Reduced in Diverse Mouse and Human Kidney Injuries. To determine whether loss of BCAA gene expression occurs prior to PT loss and increased creatinine levels in AAI-induced injury, we undertook qRT-PCR in C57BL/6 mice treated with a single dose of AAI and euthanized after 24 h. *Bckdhb*, *Hibch*, and *Mccc2* were already significantly down-regulated at this time-point, with other genes (e.g., *Acadm*) showing a strong trend toward down-regulation (Fig. 6*A*). To study BCAA gene expression in other mouse kidney injury models, we undertook qRT-PCR in mice treated with cisplatin (Fig. 6*B*) or subject to UUO (Fig. 6*C*). In both models, *Klf6* expression was highly up-regulated versus vehicle/controls. In cisplatin-treated mice, several of the BCAA genes tested were significantly down-regulated, with trends toward down-regulation of the other genes (Fig. 6*B*). In mice subject to UUO, all the genes tested were significantly down-regulated at both 3 and 7 d after UUO (Fig. 6*C*), suggesting that down-regulation of BCAA genes occurs early after injury.

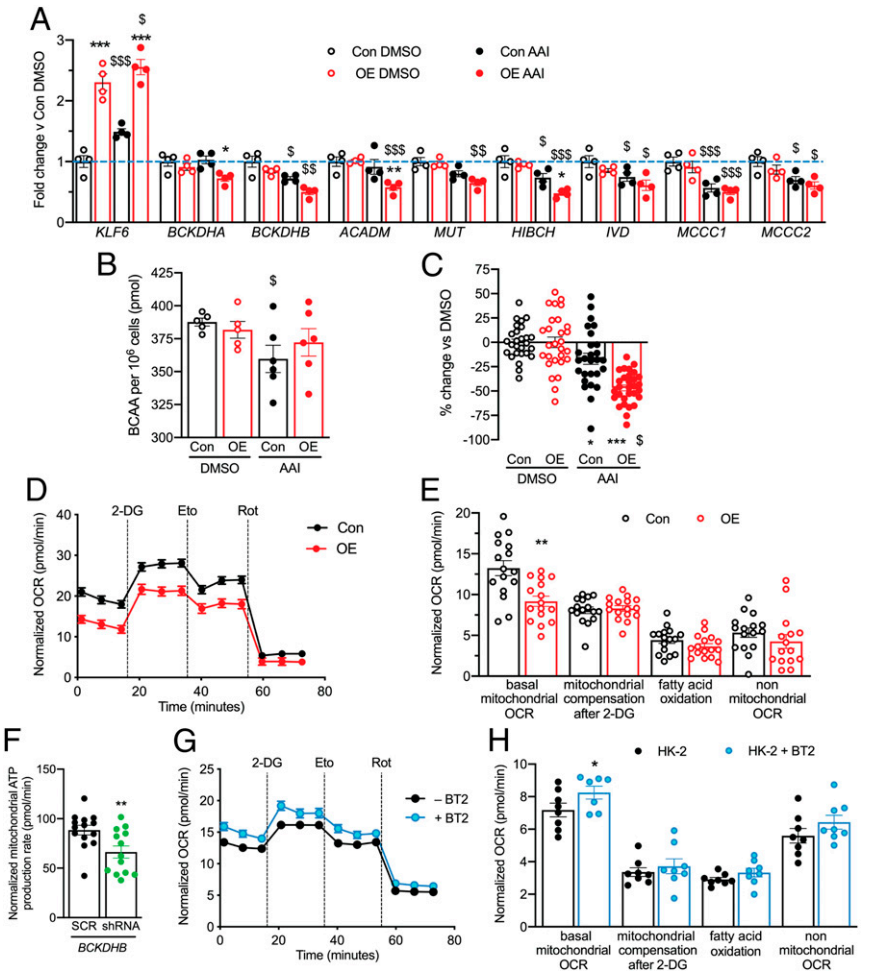

Fig. 5. KLF6 overexpression suppresses BCAA gene expression, ATP production, and BCAA utilization in vitro. (*A*) Expression of *KLF6* and BCAA metabolic genes in HK-2 cells stably expressing control (Con) or KLF6 overexpression (OE) plasmids, treated with DMSO or AAI. $n = 4$ per group; $^{*}P < 0.05$, $^{**}P < 0.01$, $^{***}P < 0.001$ versus Con AAI; $^{\$}P < 0.05$, $^{\$\$}P < 0.01$, $^{\$\$\$}P < 0.001$ versus same cell-line with DMSO; two-way ANOVA with Tukey's correction for multiple testing. (*B*) Quantification of total BCAA in Con and OE cells treated with DMSO or AAI. $n = 6$ per group; $^{\$}P < 0.05$ versus Con DMSO; one-way ANOVA with Sidak's correction for multiple testing. (*C*) Percentage change in rate of mitochondrial ATP production in Con and OE cells treated with AAI versus DMSO. $n = 27$ to 30 per group; $^{*}P < 0.05$, $^{***}P < 0.001$ versus DMSO, $^{\$}P < 0.05$ versus Con AAI; one-way ANOVA with Sidak's correction for multiple testing. (*D*) OCR measurements for Con and OE cells in restricted media. Where indicated, 2-DG, etomoxir (Eto), and a combination of rotenone/antimycin A (Rot) were added. $n = 16$ per group. (*E*) Quantifications of basal mitochondrial OCR (starting OCR minus post-Rot OCR), nonmitochondrial OCR (post-Rot OCR), and changes in OCR after adding 2-DG (mitochondrial compensation after 2-DG) and etomoxir (FAO). $n = 16$ per group; $^{**}P < 0.01$ versus Con; two-way ANOVA with Tukey's correction for multiple testing. (*F*) Mitochondrial ATP production rate in *BCKDHB*-SCR and *BCKDHB*-sh cells. $n = 14$ per group; $^{**}P < 0.05$, unpaired *t* test. (*G*) OCR measurements in HK-2 cells in restricted media in the absence or presence of BT2. Where indicated, 2-DG, Eto, and Rot were added. (*H*) Quantifications of basal mitochondrial OCR, nonmitochondrial OCR, and changes in OCR after adding 2-DG and etomoxir in HK-2 cells in the absence or presence of BT2. $n = 8$ per group; $^{*}P < 0.05$ versus no BT2; two-way ANOVA with Tukey's correction for multiple testing. Data are mean ± SEM with *n* indicating the number of biological replicates.

Similarly, data mining a previously reported expression array from the tubulointerstitial compartment of 36 human CKD patients (hypertensive and diabetic kidney diseases) compared to control patients (6) showed several BCAA genes to be downregulated in a similar manner to the AAI-treated mice (Fig. 6*D*). To further elucidate the relationship between kidney function, *KLF6* expression, and expression of BCAA genes in human CKD, we used a published expression array from the tubulointerstitial compartment of a series of 164 patients with various kidney diseases (29). Ranking of patients by eGFR showed a significant inverse correlation between eGFR and *KLF6* expression and a significant positive correlation between eGFR and each BCAA gene expression, with significant inverse correlations also between *KLF6* and each BCAA gene expression (Fig. 6*E*). Indeed, even individuals with only moderate decreases in eGFR (~45 to 60 mL/min/1.73m^2) had significantly increased expression of *KLF6* and decreased BCAA gene expression compared to individuals with normal eGFR (>90 mL/min/1.73m^2) ($P < 0.001$ for all genes), demonstrating that these alterations in gene expression may occur early in relation to functional changes. Collectively, these data suggest that KLF6-mediated suppression of genes critical to BCAA catabolism might play a critical role in exacerbating kidney injury in murine models of kidney fibrosis as well as in human CKD.

Discussion

In this study, we demonstrate the in vivo role of PT-specific KLF6 in the setting of kidney injury. KLF6 is strongly and consistently upregulated early in the PT in response to kidney injury, but this is a maladaptive response, as demonstrated by the protective effect of loss of PT *Klf6* after treatment with the clinically relevant and highly PT-specific toxin AAI. In addition, we demonstrate the

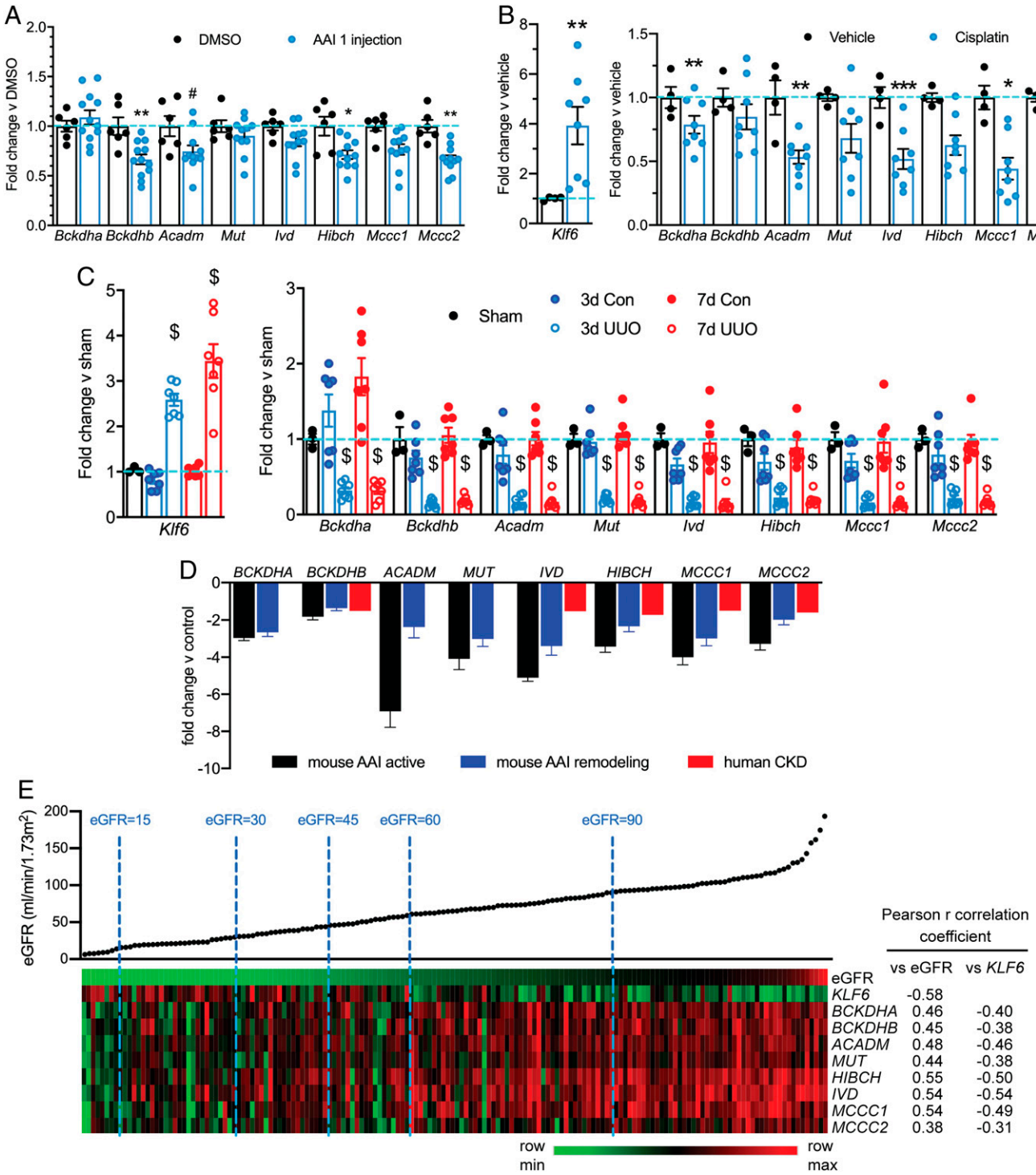

Fig. 6. BCAA gene expression is reduced in mouse and human kidney disease of diverse origins. (*A*) BCAA gene expression in kidney cortex from mice treated with one injection of AAI and euthanized 24 h later. $n = 6$ to 11 per group; $^{\#}P = 0.051$, $^{*}P < 0.05$, $^{**}P < 0.01$ versus DMSO; two-way ANOVA with Sidak's correction for multiple testing. (*B*) *Klf6* and BCAA gene expression in kidney cortex from mice treated with cisplatin. $n = 4$ to 8 per group; $^{*}P < 0.05$, $^{**}P < 0.01$, $^{***}P < 0.001$ versus vehicle; two-way ANOVA with Sidak's correction for multiple testing. (*C*) *Klf6* and BCAA gene expression in kidney cortex from mice subject to sham surgery and UUO. $n = 3$ to 7 per group; $^{\$}P < 0.001$ versus sham and contralateral control (Con); two-way ANOVA with Tukey's correction for multiple testing. (*D*) BCAA gene expression in active and remodeling phase AAI-treated versus DMSO-treated mice from RNA-seq data ($n = 3$ mice per group) and the tubulointerstitial compartment of 36 human patients with CKD compared to control patients (6). Adjusted *P* value is <0.01 for all mice data and <0.05 for human data. (*A*–*D*) Data are mean ± SEM with *n* indicating the number of biological replicates. (*E*) Correlation between eGFR, *KLF6*, and BCAA gene expression using expression array data from the tubulointerstitial compartment of 164 human kidney disease patients (29). Each dot in the graph and column in the heatmap represents an individual patient, ranked by eGFR. Pearson r correlation coefficients for expression of each gene versus eGFR and for *KLF6* versus each BCAA gene expression are shown, $P < 0.001$ for all (two-tailed).

potential significance of dysregulated BCAA metabolism in injured PT as a possible contributor to AKI and ensuing fibrosis. The loss of *Klf6* led to preservation of BCAA catabolic enzyme expression, with several of the genes encoding these enzymes having KLF6 binding sites in close proximity to their TSSs, suggesting that KLF6 may be a transcriptional suppressor of BCAA catabolism. Although another member of the KLF family, KLF15, has been previously shown to regulate skeletal muscle branched-chain aminotransferase 2 (*Bcat2*) expression (30), the regulation of other BCAA enzymes was not reported. We postulate that KLF6 acts to suppress the expression of multiple genes encoding BCAA enzymes.

In uninjured PT, *Klf6* expression is low and variably expressed in some PT cells and not others. The rapid and robust up-regulation that occurs after multiple types of injury suggests a physiologically important role for KLF6. In fibroblasts, KLF6 was recently shown to be up-regulated in response to both oncogenic and oxidative stress, leading to cellular senescence, while silencing of KLF6 led to accumulation of markers of DNA damage and genomic instability (31). Thus, the physiological role of KLF6 in injury may be induction of cellular senescence, allowing repair of DNA damage that may result from toxic or oxidative/ischemic insults. However, in injured PT cells, a second consequence of *Klf6* up-regulation appears to be suppression of BCAA catabolism which in PT cells particularly is likely detrimental. Interestingly, despite the partial knockdown of PT-specific *Klf6* at baseline in *Klf6*^{PTKD} mice, this was still able to confer a clear protective effect after injury. This has important therapeutic implications, as it suggests that only a small manipulation in KLF6 levels or activity (e.g., through use of a small molecule inhibitor) could show therapeutic efficacy. Indeed, transcription factors are more likely than other gene families in the human genome to have dosage sensitivity (32). Similarly, one limitation of our inducible KLF6 overexpression murine model is that it is not restricted PT cells, and as such, future studies will need to focus on using a cell-specific–inducible model to elucidate the cell context–dependent role of KLF6.

We previously demonstrated that loss of *Klf6* in glomerular podocytes was detrimental in the setting of FSGS due to its role in transcriptional activation of synthesis of cytochrome *c* oxidase 2 (*Sco2*). Loss of *Klf6* in FSGS led to worse fibrosis, with increased activation of the intrinsic apoptotic pathway (15). Interrogation of available single-cell RNA-seq datasets shows that in healthy mouse kidneys, *Klf6* is expressed in a much greater proportion of podocytes than PT cells, and at a much higher level (ref. 33; https://susztaklab.com/). KLF6 therefore likely plays a more important physiological role in normal podocytes than PT cells, whereas other known mitochondrial master regulators (e.g., *Ppara*) are expressed much more highly in PT cells than podocytes. Thus, loss of *Klf6* in podocytes therefore likely has a more detrimental effect than in PT cells. The contrasting roles of KLF6 in different cell types within the kidney parallels previous findings of cell-specific effects in heart and liver. Thus, knockdown of *Klf6* in cardiac myocytes in mice attenuated cardiac fibrosis after an angiotensin II overload, suggesting a role for KLF6 in propagating fibrosis, but knockdown of *Klf6* in cardiac myofibroblasts had no effect on fibrosis (14). Conversely, in liver, knockdown of *Klf6* in mouse hepatocytes had no effect on hepatic fibrosis after chronic CCl_4 administration, but overexpression of *KLF6* in hepatic stellate cells resulted in decreased fibrosis, suggesting that KLF6 is protective (13).

Loss of FAO during kidney injury is now known to be an important event in the pathology of kidney injury and indeed can directly contribute to fibrosis. In the absence of FAO, which is the main energy source for uninjured PT, other potential energy sources may assume greater importance. BCAAs contribute to the TCA cycle through production of acetyl-CoA and succinyl-CoA. A recent study demonstrated that not only do ^{13}C-labeled BCAA contribute to TCA cycle intermediates in the kidney but the kidney had the fourth-highest incorporation of ^{13}C into TCA cycle intermediates of the organs tested, after pancreas, muscle, and white adipose tissue (34), suggesting that BCAA are potentially an important contributor to the TCA cycle. However, the significance of BCAA catabolism in contributing to the TCA cycle, either in normal or injured kidneys, has not been previously explored. For example, it is not known whether loss of PT BCAA catabolism alone would cause changes in PT homeostasis and/or repair, and these studies will require generation of novel mouse models such as PT-specific *Bckdhb* knockdown mice. In the setting of kidney injury, when FAO is severely suppressed, additional suppression of genes encoding BCAA metabolic enzymes may deprive tubular cells of an important alternative potential energy source. It is important to note that BCAA gene expression was already downregulated 24 h after a single injection, prior to any changes in serum creatinine or PT loss, indicating that these downregulations were a specific consequence of PT injury and not linked to decreased PT energy demand resulting from reduced GFR and consequent reduced requirement for solute uptake. These pathways were preserved in *Klf6*^{PTKD} mice which were protected from injury and further suppressed in h*KLF6*^{OE} mice which had worse injury. In addition, *KLF6*-OE cells had reduced mitochondrial ATP production after AAI treatment compared to *KLF6*-Con cells, and while intracellular BCAA were reduced in *KLF6*-Con cells, consistent with their catabolism, this decrease was not detected in *KLF6*-OE cells. Furthermore, knockdown of *BCKDHB* in HK-2 cells resulted in decreased mitochondrial ATP production. Thus, preserved expression of BCAA genes in *Klf6*^{PTKD} mice may provide protection against injury by supplying vital TCA cycle intermediates in the setting of severely reduced FA oxidation. Future studies using mice with genetic manipulations of BCAA catabolism and/or treatment with BT2 would enable us to investigate the dynamic between BCAA catabolism and FAO in kidney injury.

We have shown that loss of expression of BCAA genes leads to decreased mitochondrial respiration and ATP production, and this represents one mechanism by which loss of BCAA catabolism may contribute to kidney injury. An alternative mechanism could be through accumulation of BCAA, which may have a toxic effect. Indeed, this has been shown in the setting of cardiac IRI. Accumulation of BCAA due to loss of catabolism was shown to inhibit mitochondrial pyruvate utilization by posttranslationally inactivating pyruvate dehydrogenase, thus removing a further cellular energy source and exacerbating injury (35). This was reversed either by increasing BCAA catabolism by treating the mice with BT2 or by increasing glucose metabolism by overexpression of GLUT1. A recent study also showed exacerbation of cardiac IRI by loss of BCAA catabolism in diabetic mice. This was accompanied by increased oxidative stress and again was reversed by reactivation of BCAA catabolism (36). BCAA and in particular leucine are known to activate mammalian target of rapamycin (mTOR) complex 1 (mTORC1) signaling. In a mouse model of polycystic kidney disease, in which cells surrounding cysts have activation of mTOR signaling, supplementation with BCAA further activated mTORC1 signaling, leading to increased proliferation (37). Transcriptional profiling of hepatocellular carcinomas revealed decreased BCAA gene expression, leading to accumulation of BCAA in tumor tissue. This was associated with increased mTORC1 signaling and proliferation, which was reduced by restricting BCAAs or treating with BT2, and was exacerbated in mice fed a high BCAA diet (38). mTORC1 signaling is required for PT function, and studies using mTOR inhibitors in kidney injury have shown conflicting results, likely due to different dosing regimens, timing of treatments, and injury models (39–42). mTORC1 signaling leads to a multitude of cellular responses, including cell growth and proliferation, lipid synthesis, mitochondrial synthesis and suppression of autophagy (43). It is likely that either under- or overactivation of mTORC1 signaling could be detrimental and that a balance is required for

correct cellular function. For example, overactivation of mTORC1 signaling in PT injury may lead to detrimental suppression of autophagy, which is required for removal of damaged mitochondria, and has been shown to be important for recovery after PT injury (39, 42, 44, 45). Thus, accumulation of leucine may have a detrimental role in kidney injury by overactivation of mTORC1 signaling and suppression of autophagy.

In conclusion, we have shown that the robust up-regulation of *Klf6* that occurs in kidney injury is detrimental, in which the loss of PT-specific *Klf6* preserved BCAA gene expression and attenuated AKI and eventual fibrosis. Conversely, induction of *KLF6* in mice suppressed BCAA gene expression and rendered the kidney susceptible to kidney injury. Furthermore, genes encoding multiple BCAA enzymes have KLF6 binding sites, suggesting that KLF6 may be a transcriptional regulator of BCAA catabolism. Down-regulation of BCAA catabolism in vitro by overexpression of KLF6 and treatment with AAI, or by knockdown of *BCKDHB*, led to decreased mitochondrial ATP production. Collectively, these data suggest that therapeutically targeting the preservation of BCAA catabolism may provide an alternative mitochondrial energy source in the setting of kidney injury in which FAO is reduced.

Concise Methods

In Vivo Studies. Control ($Klf6^{fl/fl}$) and PT-specific *Klf6* knockdown ($Klf6^{PTKD}$) or control and KLF6-overexpressing ($hKLF6^{OE}$) mice were treated with multiple doses of AAI or cisplatin or subject to UUO. DNA-AL adducts were quantified by postlabeling assay (46). Kidney injury was assessed by serum creatinine and urea nitrogen measurements, histological scoring by a pathologist, and immunofluorescent staining and quantification for markers of PT, fibrosis, and inflammation. RNA-seq was undertaken on microdissected PT segments or kidney cortex using TruSeq Stranded mRNA Sample Preparation kit (Illumina) to generate complementary DNA (cDNA) libraries, which were sequenced on a HiSeq 4000 sequencer (Illumina). Differentially expressed genes were determined using the limma method. Significantly differentially expressed genes were defined as having a >1.5- or <0.67-fold change and Benjamini–Hochberg-adjusted *P* value of <0.05. KLF6 binding site data were obtained from deposited ChIP-Seq data (accession GSE96355), and locations of binding sites were determined using the Genomic Regions Enrichment of Annotations Tool (47). qPCR was undertaken using SYBR green fluorescence.

In Vitro Studies. HK-2 cells with overexpression of *KLF6* or knockdown of *BCKDHB* and appropriate control cell-lines were generated using lentiviral infection. Cells were treated with DMSO (vehicle) or 25 μM AAI for 6 h (gene expression) or 24 h (metabolic assays). Oxygen consumption and extracellular acidification rates were measured using a Seahorse XFe96 Analyzer (Agilent) in the presence or absence of mitochondrial function inhibitors. Cellular BCAA content was measured using a colorimetric assay kit (Biovision).

Data Availability. RNA-seq data have been deposited in the Gene Expression Omnibus (GSE150656, GSE150897).

ACKNOWLEDGMENTS. This work was supported by funds from the University of Alabama at Birmingham–University of California San Diego O'Brien Center (Award P30DK079337 from the National Institute of Diabetes and Digestive and Kidney Diseases) and an American Society of Nephrology KidneyCure Joseph V. Bonventre Research Scholar Grant to S.E.P.; the Zickler Foundation, the Henry and Marsha Laufer Foundation, and National Institute for Environmental Health Sciences (1R56ES029514-01A1) to V.S.S.; NIH/National Institute for Environmental Health Sciences (DK112984, DK121846), Veterans Affairs Merit (1I01BX003698), and Dialysis Clinic, Inc. to S.K.M.; and NIH Grants (U54HL127624 and U24CA224260) to A.M. We would like to thank Dr. W. Lieberthal for supplying the samples from cisplatin-treated mice.

1. B. C. Liu, T. T. Tang, L. L. Lv, H. Y. Lan, Renal tubule injury: A driving force toward chronic kidney disease. *Kidney Int.* **93**, 568–579 (2018).
2. M. Chang-Panesso *et al.*, FOXM1 drives proximal tubule proliferation during repair from acute ischemic kidney injury. *J. Clin. Invest.* **129**, 5501–5517 (2019).
3. D. Zhou *et al.*, Tubule-derived wnts are required for fibroblast activation and kidney fibrosis. *J. Am. Soc. Nephrol.* **28**, 2322–2336 (2017).
4. D. Zhou *et al.*, Sonic hedgehog is a novel tubule-derived growth factor for interstitial fibroblasts after kidney injury. *J. Am. Soc. Nephrol.* **25**, 2187–2200 (2014).
5. L. Yang, T. Y. Besschetnova, C. R. Brooks, J. V. Shah, J. V. Bonventre, Epithelial cell cycle arrest in G2/M mediates kidney fibrosis after injury. *Nat. Med.* **16**, 535–543 (2010).
6. H. M. Kang *et al.*, Defective fatty acid oxidation in renal tubular epithelial cells has a key role in kidney fibrosis development. *Nat. Med.* **21**, 37–46 (2015).
7. T. Chiba *et al.*, Sirtuin 5 regulates proximal tubule fatty acid oxidation to protect against AKI. *J. Am. Soc. Nephrol.* **30**, 2384–2398 (2019).
8. J. Liu *et al.*, Molecular characterization of the transition from acute to chronic kidney injury following ischemia/reperfusion. *JCI Insight* **2**, e94716 (2017).
9. P. E. Cippà *et al.*, Transcriptional trajectories of human kidney injury progression. *JCI Insight* **3**, e123151 (2018).
10. H. Wu, C. F. Lai, M. Chang-Panesso, B. D. Humphreys, Proximal tubule translational profiling during kidney fibrosis reveals proinflammatory and long noncoding RNA expression patterns with sexual dimorphism. *J. Am. Soc. Nephrol.* **31**, 23–38 (2020).
11. M. J. Rane, Y. Zhao, L. Cai, Krüppel-like factors (KLFs) in renal physiology and disease. *EBioMedicine* **40**, 743–750 (2019).
12. V. Andreoli, R. C. Gehrau, J. L. Bocco, Biology of Krüppel-like factor 6 transcriptional regulator in cell life and death. *IUBMB Life* **62**, 896–905 (2010).
13. Z. Ghiassi-Nejad *et al.*, Reduced hepatic stellate cell expression of Kruppel-like factor 6 tumor suppressor isoforms amplifies fibrosis during acute and chronic rodent liver injury. *Hepatology* **57**, 786–796 (2013).
14. D. Sawaki *et al.*, Modulation of cardiac fibrosis by Krüppel-like factor 6 through transcriptional control of thrombospondin 4 in cardiomyocytes. *Cardiovasc. Res.* **107**, 420–430 (2015).
15. S. K. Mallipattu *et al.*, Krüppel-like factor 6 regulates mitochondrial function in the kidney. *J. Clin. Invest.* **125**, 1347–1361 (2015).
16. J. Holian *et al.*, Role of Kruppel-like factor 6 in transforming growth factor-beta1-induced epithelial-mesenchymal transition of proximal tubule cells. *Am. J. Physiol. Renal Physiol.* **295**, F1388–F1396 (2008).
17. M. S. Banck *et al.*, KLF6 degradation after apoptotic DNA damage. *FEBS Lett.* **580**, 6981–6986 (2006).
18. I. Jadot, A. E. Declèves, J. Nortier, N. Caron, An integrated view of aristolochic acid nephropathy: Update of the literature. *Int. J. Mol. Sci.* **18**, 297 (2017).
19. L. Huang, A. Scarpellini, M. Funck, E. A. Verderio, T. S. Johnson, Development of a chronic kidney disease model in C57BL/6 mice with relevance to human pathology. *Nephron Extra* **3**, 12–29 (2013).
20. K. G. Dickman, D. H. Sweet, R. Bonala, T. Ray, A. Wu, Physiological and molecular characterization of aristolochic acid transport by the kidney. *J. Pharmacol. Exp. Ther.* **338**, 588–597 (2011).
21. S. K. Mallipattu, C. C. Estrada, J. C. He, The critical role of Krüppel-like factors in kidney disease. *Am. J. Physiol. Renal Physiol.* **312**, F259–F265 (2017).
22. H. Wu, Y. Kirita, E. L. Donnelly, B. D. Humphreys, Advantages of single-nucleus over single-cell RNA sequencing of adult kidney: Rare cell types and novel cell states revealed in fibrosis. *J. Am. Soc. Nephrol.* **30**, 23–32 (2019).
23. H. Wu *et al.*, Single-cell transcriptomics of a human kidney allograft biopsy specimen defines a diverse inflammatory response. *J. Am. Soc. Nephrol.* **29**, 2069–2080 (2018).
24. C. C. Leow *et al.*, Prostate-specific Klf6 inactivation impairs anterior prostate branching morphogenesis through increased activation of the Shh pathway. *J. Biol. Chem.* **284**, 21057–21065 (2009).
25. E. B. Rankin, J. E. Tomaszewski, V. H. Haase, Renal cyst development in mice with conditional inactivation of the von Hippel-Lindau tumor suppressor. *Cancer Res.* **66**, 2576–2583 (2006).
26. R. Lan *et al.*, Mitochondrial pathology and glycolytic shift during proximal tubule atrophy after ischemic AKI. *J. Am. Soc. Nephrol.* **27**, 3356–3367 (2016).
27. Y. Li *et al.*, Evolution of altered tubular metabolism and mitochondrial function in sepsis-associated acute kidney injury. *Am. J. Physiol. Renal Physiol.* **319**, F229–F244 (2020).
28. M. Neinast, D. Murashige, Z. Arany, Branched chain amino acids. *Annu. Rev. Physiol.* **81**, 139–164 (2019).
29. W. Ju *et al.*; ERCB, C-PROBE, NEPTUNE, and PKU-IgAN Consortium, Tissue transcriptome-driven identification of epidermal growth factor as a chronic kidney disease biomarker. *Sci. Transl. Med.* **7**, 316ra193 (2015).
30. S. Gray *et al.*, Regulation of gluconeogenesis by Krüppel-like factor 15. *Cell Metab.* **5**, 305–312 (2007).
31. M. E. Sabatino *et al.*, Krüppel-like factor 6 is required for oxidative and oncogene-induced cellular senescence. *Front. Cell Dev. Biol.* **7**, 297 (2019).
32. Z. Ni, X. Y. Zhou, S. Aslam, D. K. Niu, Characterization of human dosage-sensitive transcription factor genes. *Front. Genet.* **10**, 1208 (2019).
33. J. Park *et al.*, Single-cell transcriptomics of the mouse kidney reveals potential cellular targets of kidney disease. *Science* **360**, 758–763 (2018).
34. M. D. Neinast *et al.*, Quantitative analysis of the whole-body metabolic fate of branched-chain amino acids. *Cell Metab.* **29**, 417–429.e4 (2019).
35. T. Li *et al.*, Defective branched-chain amino acid catabolism disrupts glucose metabolism and sensitizes the heart to ischemia-reperfusion injury. *Cell Metab.* **25**, 374–385 (2017).
36. K. Lian *et al.*, PP2Cm overexpression alleviates MI/R injury mediated by a BCAA catabolism defect and oxidative stress in diabetic mice. *Eur. J. Pharmacol.* **866**, 172796 (2020).
37. J. Yamamoto *et al.*, Branched-chain amino acids enhance cyst development in autosomal dominant polycystic kidney disease. *Kidney Int.* **92**, 377–387 (2017).

38. R. E. Ericksen *et al*., Loss of BCAA catabolism during carcinogenesis enhances mTORC1 activity and promotes tumor development and progression. *Cell Metab.* **29**, 1151–1165.e6 (2019).
39. M. Jiang *et al*., Autophagy in proximal tubules protects against acute kidney injury. *Kidney Int.* **82**, 1271–1283 (2012).
40. W. Lieberthal *et al*., Rapamycin impairs recovery from acute renal failure: Role of cell-cycle arrest and apoptosis of tubular cells. *Am. J. Physiol. Renal Physiol.* **281**, F693–F706 (2001).
41. S. L. Lui *et al*., Effect of rapamycin on renal ischemia-reperfusion injury in mice. *Transpl. Int.* **19**, 834–839 (2006).
42. S. Sunahara *et al*., Influence of autophagy on acute kidney injury in a murine cecal ligation and puncture sepsis model. *Sci. Rep.* **8**, 1050 (2018).
43. D. Fantus, N. M. Rogers, F. Grahammer, T. B. Huber, A. W. Thomson, Roles of mTOR complexes in the kidney: Implications for renal disease and transplantation. *Nat. Rev. Nephrol.* **12**, 587–609 (2016).
44. S. Liu *et al*., Autophagy plays a critical role in kidney tubule maintenance, aging and ischemia-reperfusion injury. *Autophagy* **8**, 826–837 (2012).
45. A. Takahashi *et al*., Autophagy guards against cisplatin-induced acute kidney injury. *Am. J. Pathol.* **180**, 517–525 (2012).
46. V. S. Sidorenko *et al*., Lack of recognition by global-genome nucleotide excision repair accounts for the high mutagenicity and persistence of aristolactam-DNA adducts. *Nucleic Acids Res.* **40**, 2494–2505 (2012).
47. C. Y. McLean *et al*., GREAT improves functional interpretation of cis-regulatory regions. *Nat. Biotechnol.* **28**, 495–501 (2010).